Supporting information

Synthesis, structure and temperature sensing of lanthanide-organic framework constructed from a pyridine-containing tetracarboxylic acid ligand

Dian Zhao,[ab*] Huizhen Wang,[b] and Guodong Qian[b*]

a Key Laboratory of the Ministry of Education for Advanced Catalysis Materials, Department of Chemistry, Zhejiang Normal University, Jinhua, 321004, China.
b State Key Laboratory of Silicon Materials, Cyrus Tang Center for Sensor Materials and Applications, School of Materials Science and Engineering, Zhejiang University, Hangzhou 310027, China.

*Corresponding Author:
dzhao@zjnu.edu.cn; gdqian@zju.edu.cn;

Table S1 Comparing the performance of the LnMOF thermometers in terms of temperature range, relative sensitivity (S_r) at high temperatures.

MOF	Range (K)	S_r (%K^{-1})	T (K)	Ref
$Eu_{0.19}Tb_{0.81}$PDDI	313~473	0.37	473	This work
$[Eu_{0.7}Tb_{0.3}$(D-cam)$(Himdc)_2(H_2O)_2]_3$	100~450	0.11	450	1
$Eu_{0.37}Tb_{0.63}$-BTC-a	313~473	0.17	473	2
Eu@UIO-66-Hybrid film	303~403	2.11	403	3
Dycpia	298~473	0.42	473	4

Table S2. Crystallographic Data collection and Refinement result for **EuPDDI**.

chemical formula	$C_{21}H_6Eu_2N_3O_{18}$
formula weight	892.21
temperature (K)	293(2)
wavelength (Å)	0.71073
crystal system	Monoclinic
space group	C 2/c
a (Å)	25.132(2)
b(Å)	13.2260(8)
c (Å)	15.1630(9)
α (º)	90.000
β (º)	99.288(5)
γ (º)	90.000
V(Å3)	4974.0(6)
Z	4
density (calculated g/cm^{-3})	1.191
absorbance coefficient (mm^{-1})	2.548
F(000)	1692
goodness of fit on F_2	1.083
R1, wR2 (I>2σ(I))a	0.1069, 0.3163
R1, wR2 (all data)a	0.1143, 0.3246
largest difference peak and hole (e/$Å^3$)	6.496, -6.564

[a]$R1 = \Sigma(|Fo| - |Fc|) / \Sigma|Fo|$; $wR2 = [\Sigma w(|Fo|-|Fc|^2) / \Sigma wFo2]^{1/2}$.

Table S3 Selected Bond lengths [Å] and angles [°] for **EuPDDI**.

Eu(1)-O(3)#1	2.335(11)	O(11)#2-Eu(1)-O(6)	72.5(6)
Eu(1)-O(11)#2	2.360(12)	O(16)#3-Eu(1)-O(6)	147.5(5)
Eu(1)-O(16)#3	2.382(12)	O(1)-Eu(1)-O(6)	73.5(6)
Eu(1)-O(1)	2.398(14)	O(10)-Eu(1)-O(6)	75.8(6)
Eu(1)-O(10)	2.413(12)	O(6U)-Eu(1)-O(6)	101.4(8)
Eu(1)-O(6U)	2.442(17)	O(11)#2-Eu(1)-O(9)	70.1(6)
Eu(1)-O(6)	2.535(14)	O(16)#3-Eu(1)-O(9)	145.0(5)
Eu(1)-O(9)	2.560(17)	O(1)-Eu(1)-O(9)	101.1(7)
Eu(1)-O(3)	2.769(13)	O(10)-Eu(1)-O(9)	124.5(5)
Eu(1)-Eu(1)#1	4.0702(13)	O(6U)-Eu(1)-O(9)	70.1(7)
O(3)-Eu(1)#1	2.335(11)	O(6)-Eu(1)-O(9)	51.7(6)
O(11)-Eu(1)#4	2.360(12)	O(3)#1-Eu(1)-O(3)	74.5(4)
O(16)-Eu(1)#5	2.382(12)	O(11)#2-Eu(1)-O(3)	69.1(4)
O(3)#1-Eu(1)-O(11)#2	73.0(5)	O(16)#3-Eu(1)-O(3)	68.5(4)
O(3)#1-Eu(1)-O(16)#3	77.4(4)	O(1)-Eu(1)-O(3)	113.8(5)
O(11)#2-Eu(1)-O(16)#3	133.2(4)	O(10)-Eu(1)-O(3)	50.4(3)
O(3)#1-Eu(1)-O(1)	145.1(5)	O(6U)-Eu(1)-O(3)	140.4(6)
O(11)#2-Eu(1)-O(1)	141.8(6)	O(6)-Eu(1)-O(3)	117.8(6)
O(16)#3-Eu(1)-O(1)	75.1(5)	O(9)-Eu(1)-O(3)	138.9(6)
O(3)#1-Eu(1)-O(10)	124.2(4)	O(3)#1-Eu(1)-Eu(1)#1	41.0(3)
O(11)#2-Eu(1)-O(10)	78.9(5)	O(11)#2-Eu(1)-Eu(1)#1	65.8(3)
O(16)#3-Eu(1)-O(10)	89.1(5)	O(16)#3-Eu(1)-Eu(1)#1	68.0(3)
O(1)-Eu(1)-O(10)	76.5(5)	O(1)-Eu(1)-Eu(1)#1	138.2(5)
O(3)#1-Eu(1)-O(6U)	81.4(5)	O(10)-Eu(1)-Eu(1)#1	83.6(3)
O(11)#2-Eu(1)-O(6U)	132.4(5)	O(6U)-Eu(1)-Eu(1)#1	116.0(5)
O(16)#3-Eu(1)-O(6U)	75.9(6)	O(6)-Eu(1)-Eu(1)#1	136.2(5)
O(1)-Eu(1)-O(6U)	71.4(6)	O(9)-Eu(1)-Eu(1)#1	120.4(5)
O(10)-Eu(1)-O(6U)	147.1(5)	O(3)-Eu(1)-Eu(1)#1	33.6(2)
O(3)#1-Eu(1)-O(6)	134.8(5)	Eu(1)#1-O(3)-Eu(1)	105.5(4)

Symmetry transformations used to generate equivalent atoms: #1 -x+1/2,-y+1/2,-z+1; #2 -x+1/2,y-1/2,-z+1/2; #3 x,-y+1,z+1/2; #4 -x+1/2,y+1/2,-z+1/2; #5 x,-y+1,z-1/2.

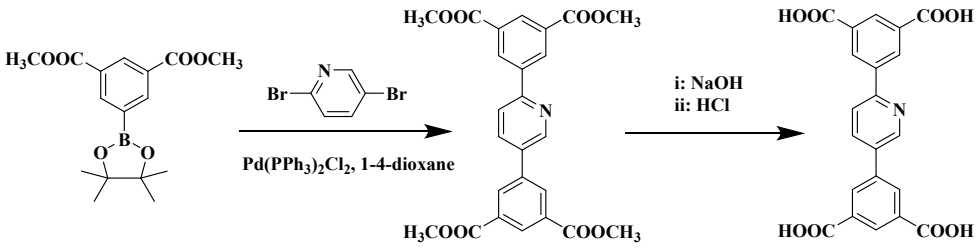

Fig. S1 Synthesis of the organic ligand H_4PDDI applied to construct **LnPDDI**.

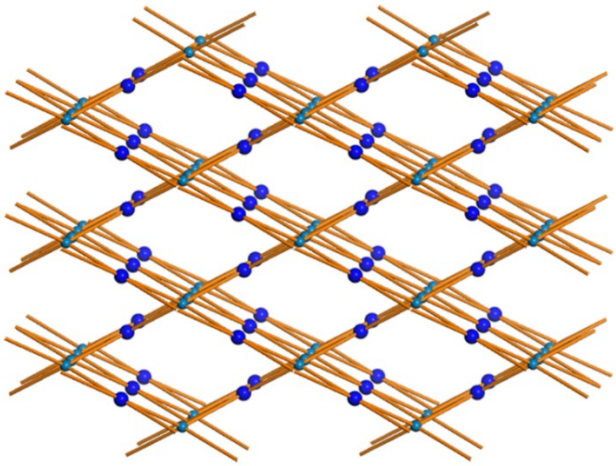

Fig. S2 The underlying network of **EuPDDI**.

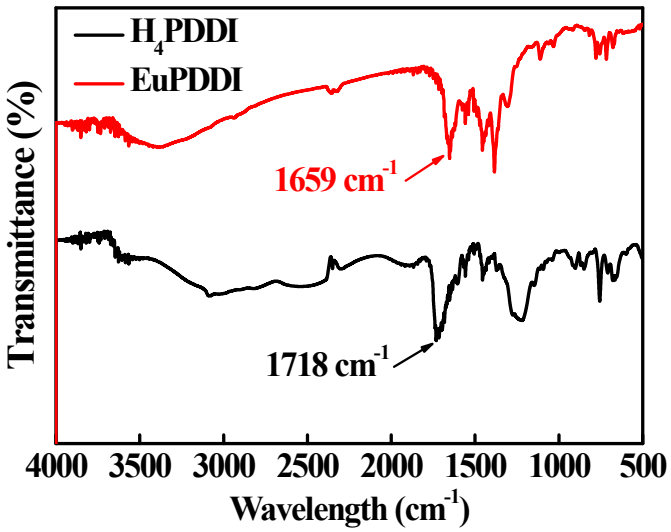

Fig. S3 FT-IR spectra of **H_4PDDI** and **EuPDDI**

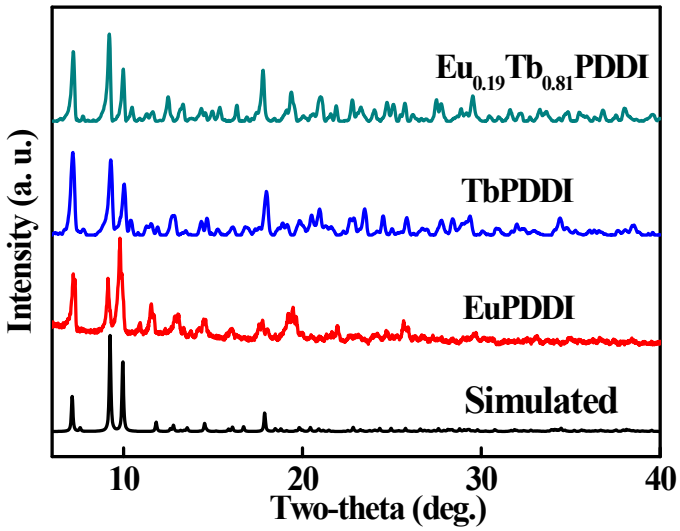

Fig. S4 Powder XRD patterns of **EuPDDI**, **TbPDDI**, **$Eu_{0.19}Tb_{0.81}$PDDI**

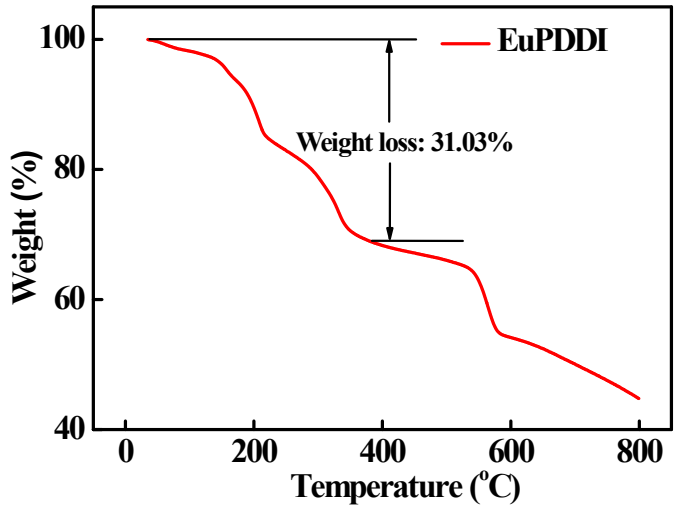

Fig. S5. TG curves of **EuPDDI**.

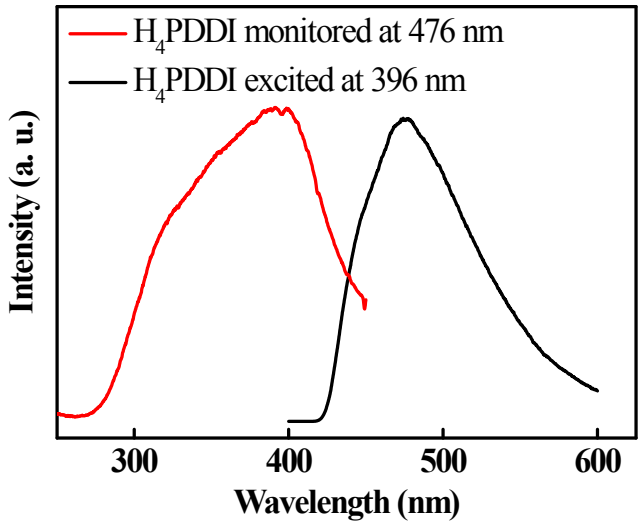

Fig. S6 Excitation and emission spectra of the H_4PDDI ligand at room temperature

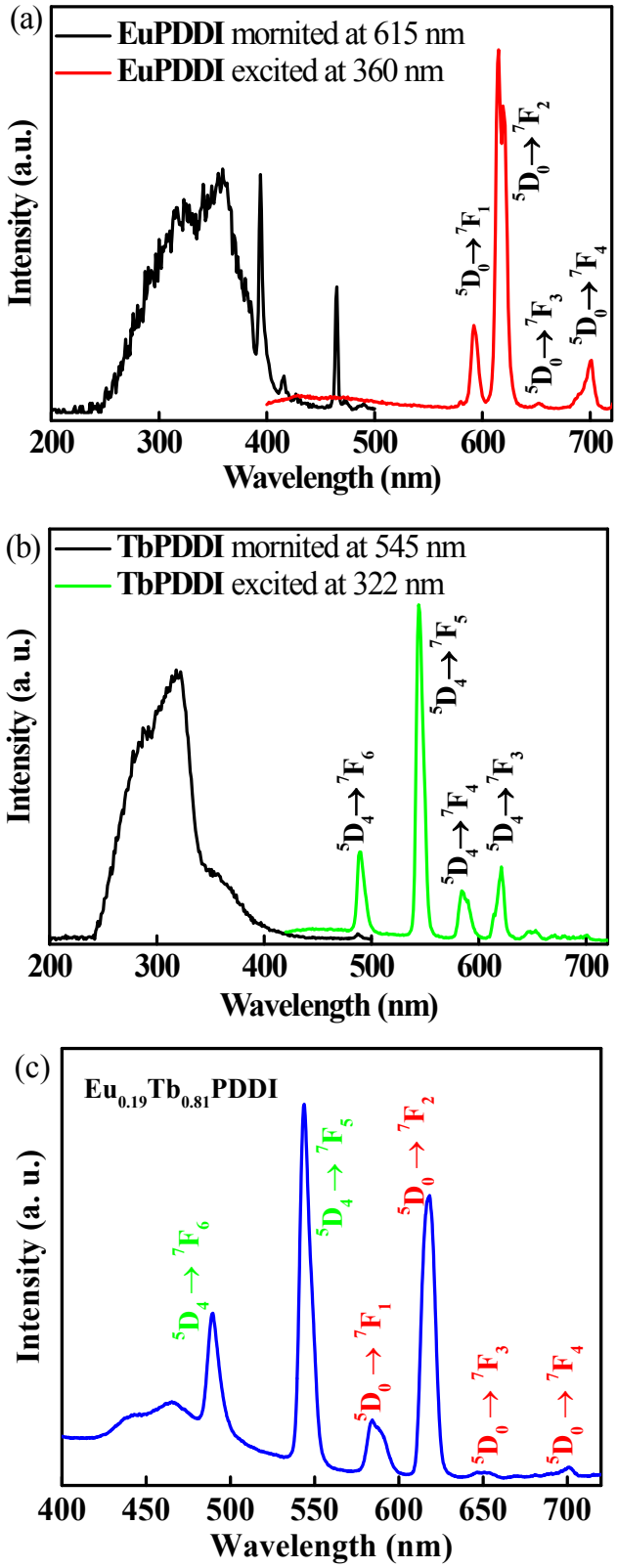

Fig. S7 (a) Excitation and emission Spectra of **EuPDDI**; (b) Excitation and emission Spectra of **TbPDDI**; (c) Excitation and emission Spectra of $\mathbf{Eu_{0.19}Tb_{0.81}PDDI}$.

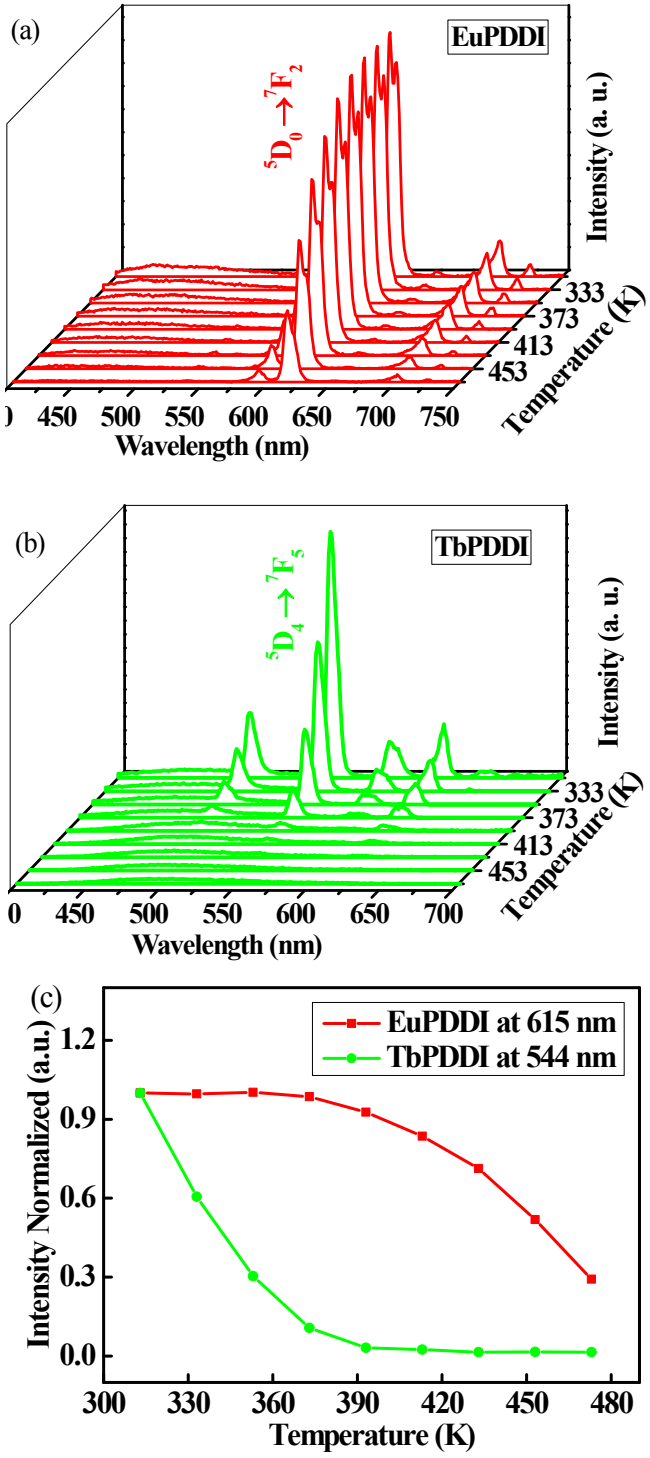

Fig. S8 (a) Temperature dependent emission spectra of **EuPDDI** recorded between 313 and 473 K; (b) Temperature dependent emission spectra of **TbPDDI** recorded between 313 and 473 K; (c) Temperature dependent normalized intensity of **EuPDDI** at 615 nm and **TbPDDI** at 544 nm recorded between 313 and 473 K.

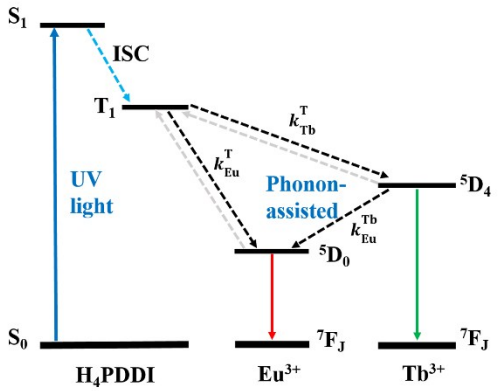

Fig. S9 Schematic representation of energy absorption, migration, emission, and processes in mixed LnMOF **$Eu_{0.19}Tb_{0.81}$PDDI**. Abbreviations: S = singlet; T = triplet; ISC = intersystem crossing; k = nonradiative and radiative transition probability. The solid arrows represent absorption and radiative transitions; dotted arrows indicate nonradiative transitions.

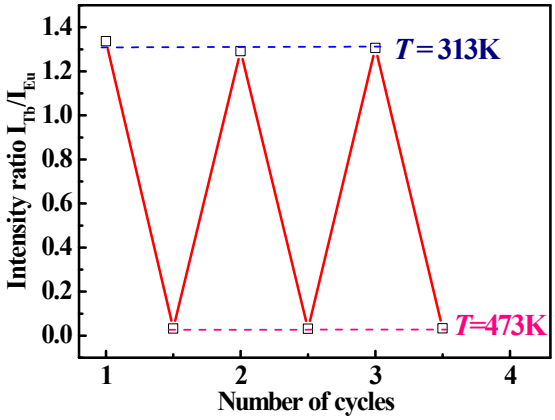

Fig. S10 The intensity ratio of Tb^{3+} (545 nm) to Eu^{3+} (615 nm) for **$Eu_{0.19}Tb_{0.81}$PDDI** in the cycles of heating and cooling (repeatability better than 98%).

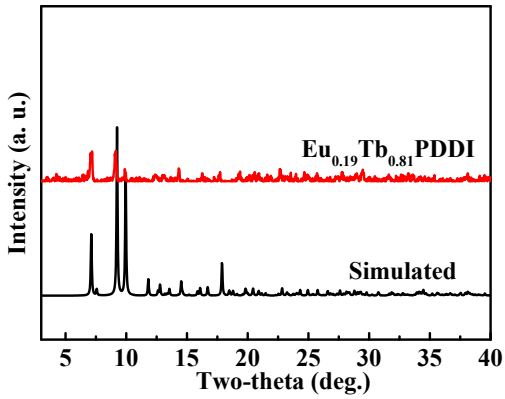

Fig. S11 Powder XRD profile of **$Eu_{0.19}Tb_{0.81}$PDDI** after high temperature photoluminescence measurements.

References

1. Y.-H. Han, C.-B. Tian, Q.-H. Li and S.-W. Du, *J. Mater. Chem. C*, 2014, **2**, 8065-8070.

2. H. Wang, D. Zhao, Y. Cui, Y. Yang and G. Qian, *J. Solid State Chem.*, 2017, **246**, 341-345.

3. J. Feng, S. Gao, T. Liu, J. Shi, and R. Cao, *ACS Appl. Mater. Interfaces*, 2018, **10**, 6014-6023.

4. T. Xia, Y. Cui, Yu Yang and G. Qian, *J. Mater. Chem. C*, 2017, **5**, 5044-5047.